

# *Cut-cells in idealised simulations*

## **Performance of the Cut-cell Method of Representing Orography in Idealised Simulations**

Beth Good<sup>1</sup>, Alan Gadian<sup>1</sup>, Sarah-Jane Lock<sup>2</sup> and Andrew N Ross<sup>3</sup>

<sup>1</sup> NCAS, University of Leeds, UK; <sup>2</sup> ECMWF, UK; <sup>3</sup> ICAS, University of Leeds, UK

# Content

1. References
2. Description of the two models used.
3. Description of the Cut-cell structure and equations used.
4. Comparison with analytical solutions for flow over an isolated bell shaped hill.
5. Resting atmosphere test.
6. Tracer bubble over a Schar mountain.
7. Rising warm bubble over an isolated hill.
8. Conclusions.

## Main references

Good B; Gadian A; Lock S-J; Ross A (2014)

Performance of the cut-cell method of representing orography in idealized simulations, *Atmospheric Science Letters*, **15**, pp.44-49.

**doi: 10.1002/asl2.465**

Lock SJ; Bitzer H-W; Coals A; Gadian A; Mobbs S (2012)

Demonstration of a cut-cell representation of 3D orography for studies of atmospheric flows over very steep hills, *Monthly Weather Review*, **140**, pp. 411-424.

**doi: 10.1175/MWR-D-11-00069.1**

Good; Gadian; Lock et al. (paper being written)

# Models used for the comparison

Model descriptions.

## 1. Cut-cell (Lock et al. 2012)

- Non-hydrostatic, 3D model (using UK UM Equation set, Davies et al. 2005).
- Predicts, winds, potential temperature and the Exner function of pressure.
- Advective form of the equations.
- Split-explicit time stepping scheme with leapfrog and forward Euler (WRF split time stepping structure).
- Centred difference advection scheme.

## 2. BLASIUS (Wood et al. 1992)

- Used for idealised studies of boundary layer flow (Gal-Chen & Somerville, 1975)
- Time-dependant Boussinesq equations.
- Explicit time integration scheme.
- Centred-difference advection scheme.
- Periodic with FFT solver.
- Turbulence closure turned off.

# Cut cell structure

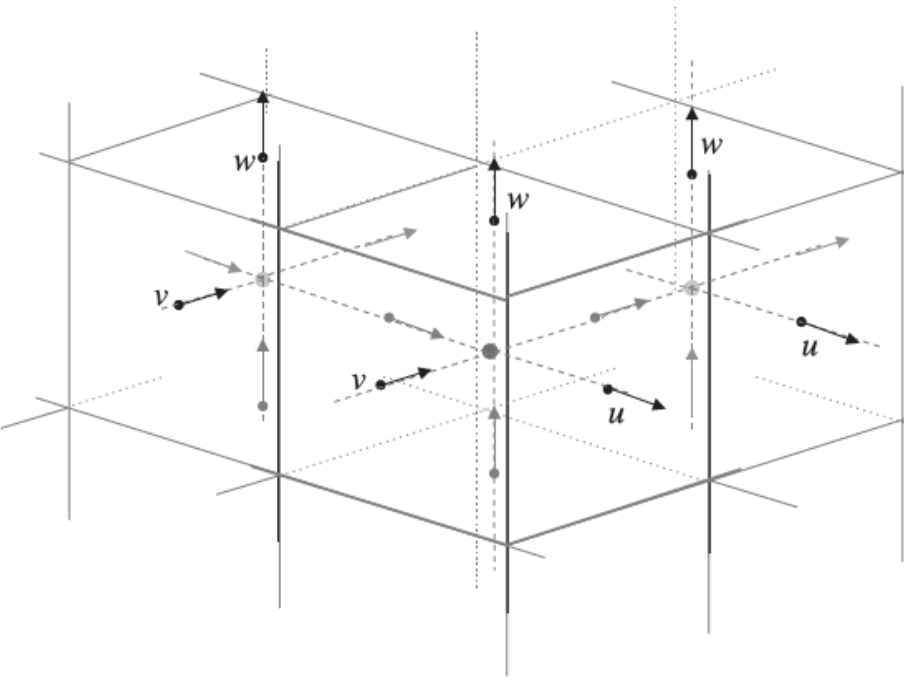


FIG. 1. Illustration of the storage locations for the model variables on a staggered grid: at the center of each grid box is stored  $\Pi'$ , denoted by a filled circle;  $u$ ,  $v$ , and  $w$  are stored on the gridbox faces perpendicular to their flow directions.

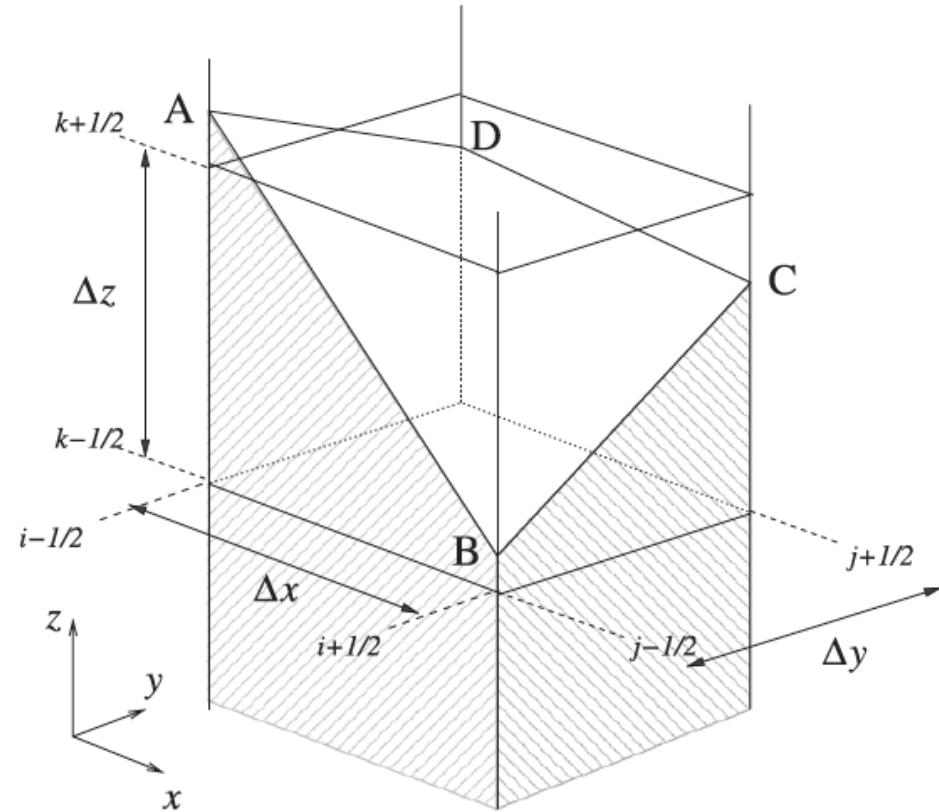


FIG. 2. The orographic heights at the four corners of the grid column centered on  $(i, j)$ —marked ABCD—define a unique bilinear surface, which results in the grid box  $(i, j, k)$  being cut by the orography.

Following Steppeler et al. (2006), 3D lower boundary is represented with piecewise bilinear surfaces. To solve the flow through the irregular shaped cut cells, an approx finite-volume approach is used (Steppeler et al. (2002) ).  $N = 3^4 - 2$  configurations.

## Cut cell equation set

$$\Pi = \bar{\Pi}(z) + \Pi'(\mathbf{x}, t),$$

$$\theta = \bar{\theta}(z) + \theta'(\mathbf{x}, t).$$

The model equations become

$$\frac{\partial u}{\partial t} + c_p \bar{\theta} \frac{\partial \Pi'}{\partial x} = -\mathbf{u} \cdot \nabla u + fv - Fw - c_p \theta' \frac{\partial \Pi'}{\partial x}, \quad (1)$$

$$\frac{\partial v}{\partial t} + c_p \bar{\theta} \frac{\partial \Pi'}{\partial y} = -\mathbf{u} \cdot \nabla v - fu - c_p \theta' \frac{\partial \Pi'}{\partial y}, \quad (2)$$

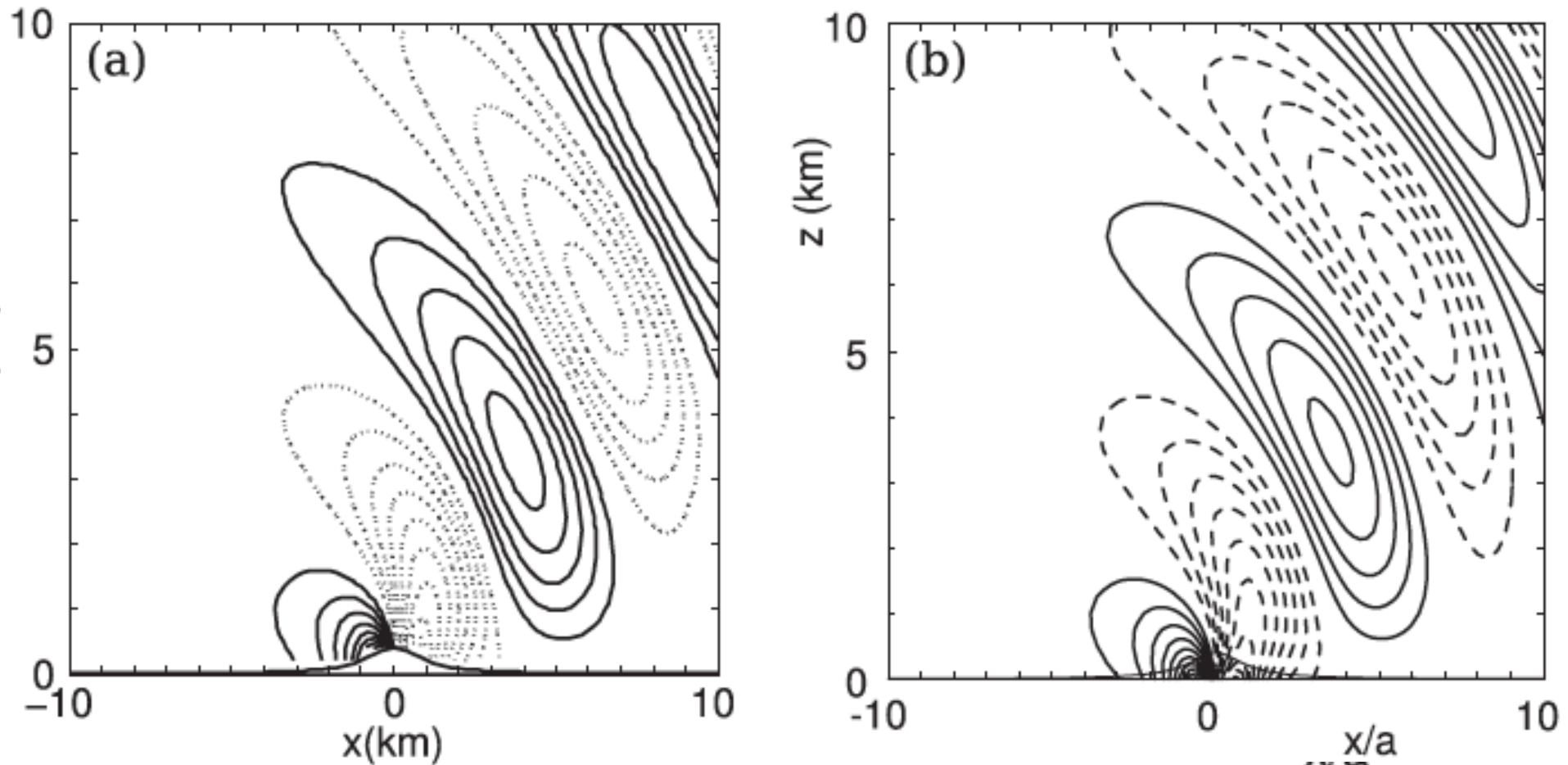
$$\frac{\partial w}{\partial t} + c_p \bar{\theta} \frac{\partial \Pi'}{\partial z} - g \frac{\theta}{\bar{\theta}} = -\mathbf{u} \cdot \nabla w + Fu - c_p \theta' \frac{\partial \Pi'}{\partial z}, \quad (3)$$

$$\frac{\partial \Pi'}{\partial t} + (\gamma - 1) \bar{\Pi} \nabla \cdot \mathbf{u} - \frac{gw}{c_p \bar{\theta}} = -\mathbf{u} \cdot \nabla \Pi' - (\gamma - 1) \Pi' \nabla \cdot \mathbf{u}, \quad (4)$$

$$\frac{\partial \theta'}{\partial t} + w \frac{\partial \bar{\theta}}{\partial z} = -\mathbf{u} \cdot \nabla \theta', \quad (5)$$



## Flow over a bell shaped hill



Comparison of the flow produced by the cut cell model and the analytic solution.  
(Gallus and Klemp 2000)

FIG. 4. Vertical velocity field for flow over a bell-shaped hill of height 400 m and half-width 1000 m, with contour interval of  $0.25 \text{ m s}^{-1}$  and positive values indicated by solid lines, negative values by dashed lines: (a) the cut-cell model results after 40 000 integrations and (b) the analytic solution for a smooth hill reproduced from (Gallus and Klemp 2000, see their Fig. 1c).

# Resting Atmosphere Test

- Simulations as in Klemp (2011)
- Periodic domain, 200km wide.
- Height = 20km high,  $d_x = 500\text{m}$
- $h_0 = 1000\text{m}$
- $a = 500\text{m}$
- $\lambda = 4000\text{m}$

Klemp (2011) showed errors due to the horizontal pressure gradient term, with an inversion amplifying the error.

The inversion was set between 2 - 3 km

$N = 0.1 \text{ s}^{-1}$   $\leq 2 \text{ km}$  and  $\geq 3\text{km}$  ; otherwise  $N = 0.2 \text{ s}^{-1}$

Run length 5 hours, time step = 1.01s

Cut Cell model .... Max vertical velocity is  **$10^{-12} \text{ m/s}$** . (**machine accuracy**) and the horizontal velocities are **zero**. Increasing hill height to 4km makes no difference.

c.f. Max vertical velocity = **1 m/s** for basic and hybrid terrain following  
= **0.1 m/s** for STF / SLEVE co-ordinates (Klemp 2011)

$$h(x) = h^*(x) \cos^2\left(\frac{\pi x}{\lambda}\right)$$

$$h^*(x) = \begin{cases} h_0 \cos^2\left(\frac{\pi x}{2a}\right) & |x| \leq a \\ 0 & |x| > a \end{cases}$$



# Advection Test

- Schar (2002) test
- Tracer bubble blown across a mountain range
- Wind,  $u(z)$  = zero below mountain tops and constant above 5km
- $u_0 = 10$  m/s ;  $z_1 = 4$ km and  $z_2 = 5$ km
- Initial tracer  $q(x,z)$  bubble has  $A_z = 3$  km ,  $A_x = 25$ km, with bubble centre  $x_0 = 100$ km ,  $z_0 = 9$ km
- Domain width = 300km; height = 25km
- $dx = 1000$ m ;  $dz = 500$ m
- $h_0 = 3000$ m ;  $a = 25$ km ;  $\lambda = 8$ km
- Neutral stability,  $\theta = 300$ K
- Run time = 10,000s ( one pass)
- Results showed no differences with no hill case.

$$q(x, z) = \begin{cases} \cos^2 \left( \frac{\pi r}{2} \right) & r \leq 1 \\ 0 & \text{otherwise} \end{cases}$$

$$r = \left[ \left( \frac{x - x_0}{A_x} \right)^2 + \left( \frac{z - z_0}{A_z} \right)^2 \right]^{\frac{1}{2}}$$

$$u(z) = \begin{cases} u_0 & z_2 \leq z \\ u_0 \sin^2 \left( \frac{\pi}{2} \frac{z - z_1}{z_2 - z_1} \right) & z_1 \leq z \leq z_2 \\ 0 & z \leq z_1 \end{cases}$$

## Results from the bubble tracer advection test

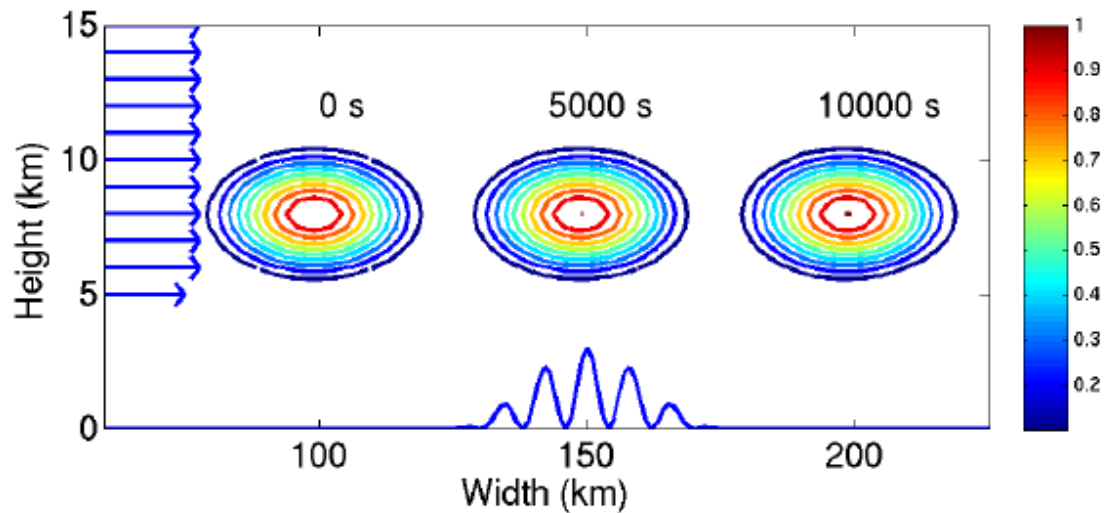


Figure 1: Results from the Cut-cell model for the advection test. Contours indicate the tracer bubble concentration according to the colourbar with intervals of 0.1 and ranging from -0.2 to 1. The position of the bubble is indicated at three times 0 s, 5,000 s and 10,000 s after the introduction of the bubble on the left. The domain shown is 150 km wide and 15 km high centred on the orography which is indicated by the blue line at the base. The vectors down the left show the wind profile, large vectors have a magnitude of  $10 \text{ m s}^{-1}$ .

## ***Conclusions from the bubble tracer advection test***

The results from the bubble advection test show:-

- The differences between the cases of orography and no orography were zero (within machine precision). This indicates that any trajectory errors are due to the advection scheme and not the terrain representation.
- Moving the bubble closer to the top of the mountains does not change the results suggestion there is no undue influence of the terrain on the flow aloft.

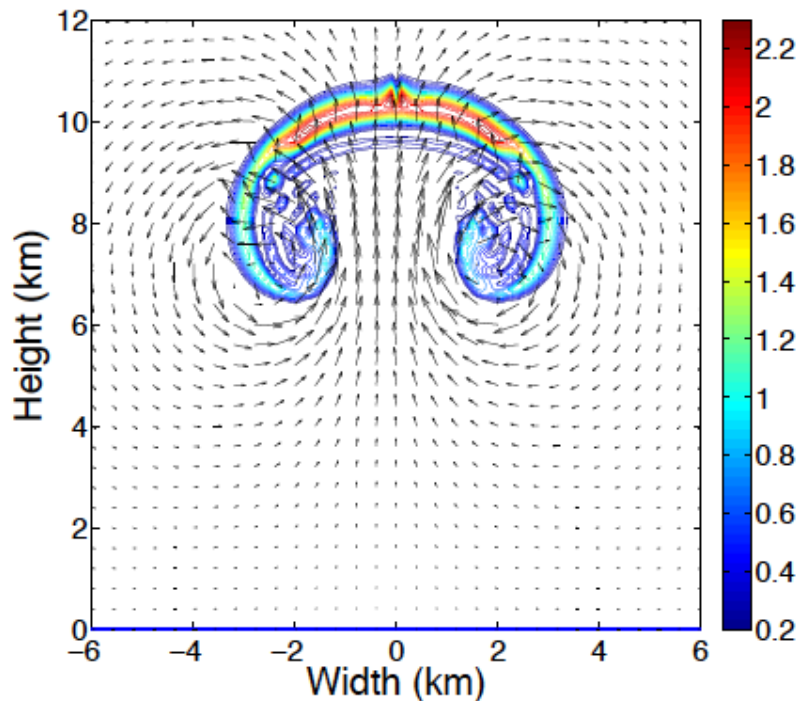
## Rising bubble, no hill case

Set up based on Bryan & Fritsch (2002). Run 1000s in time.

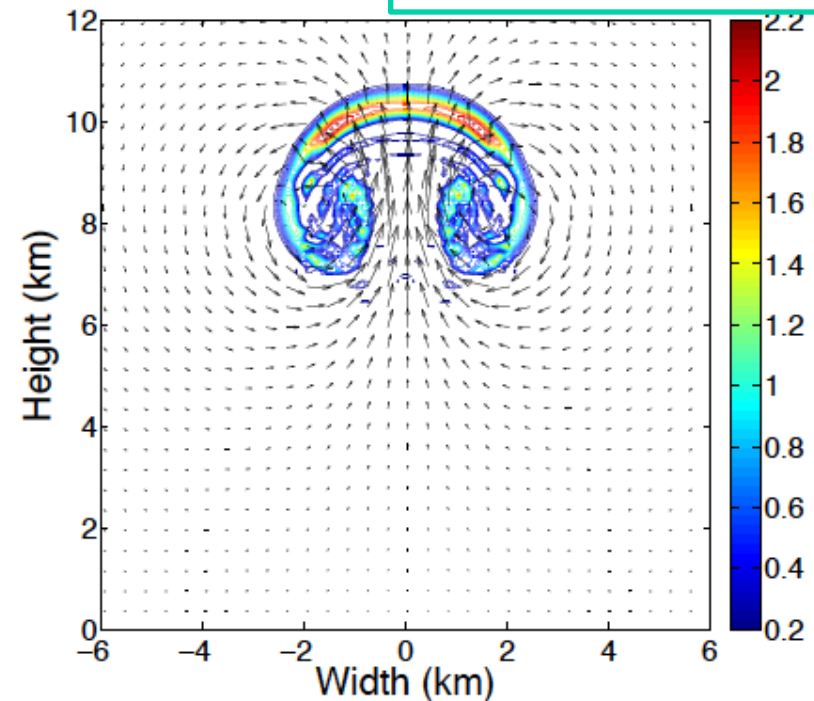
$$r = \left[ \left( \frac{x - x_0}{A_x} \right)^2 + \left( \frac{z - z_0}{A_z} \right)^2 \right]^{\frac{1}{2}} \quad \theta'(x, z) = \begin{cases} \cos^2 \left( \frac{\pi r}{2} \right) & r \leq 1 \\ 0 & \text{otherwise} \end{cases}$$

$A_z = A_x = 2\text{km}$  ;  
 $z_0 = 4.5\text{km}$  ;  
 $x_0 = 10\text{km}$   
Grid spacing = 100m  
Domain 20km\*20km  
3d model,  $N_y = 10$ .

Neutral stability  
 $\theta = 300\text{K}$



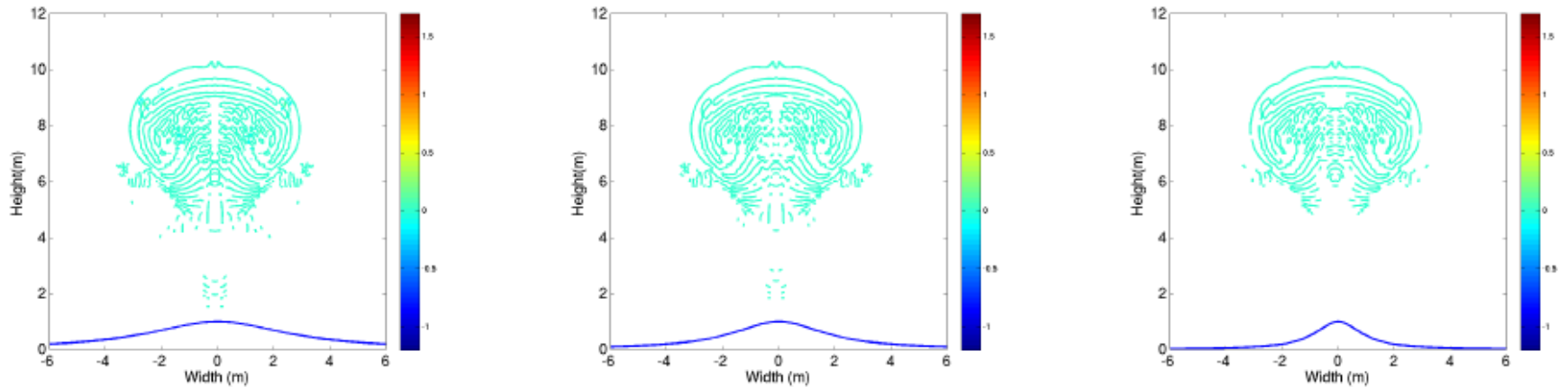
(a)



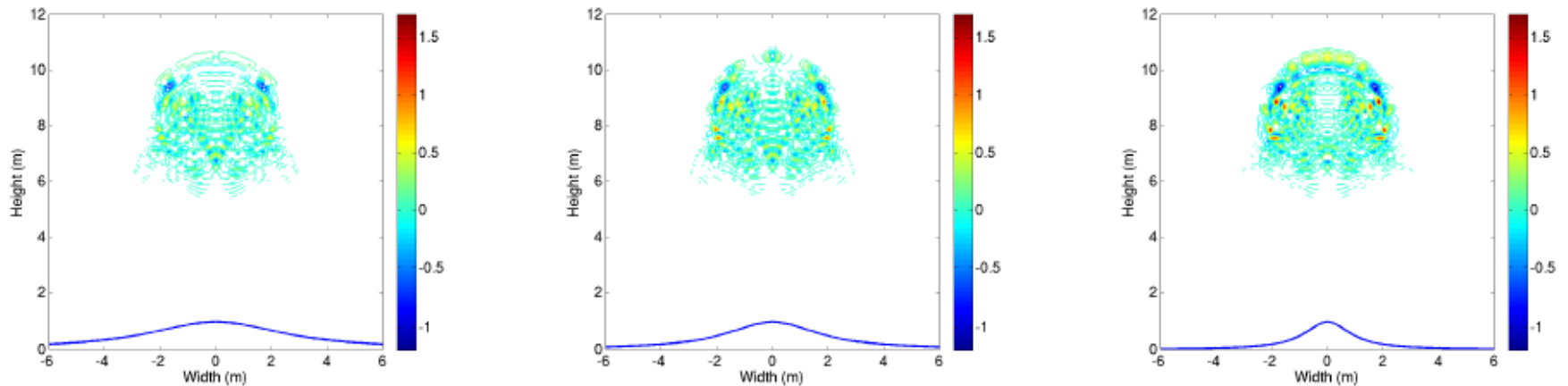
(b)

Figure 2: Potential temperature perturbations for the warm bubble after 1000 s from the Cut-cell model (a) and BLASIUS (b). The contour interval is 0.1 K. The vectors indicate the wind velocity. The maximum vertical velocity in (a) is  $15.61 \text{ m s}^{-1}$  and in (b) is  $17.17 \text{ m s}^{-1}$ .

## Rising bubble comparison (hill – no hill). Upper Row cut cell. Lower Row BLASIUS



(a) Maximum absolute difference 0.14 K. Maximum vertical velocity  $15.86 \text{ m s}^{-1}$ .  
 (b) Maximum absolute difference 0.09 K. Maximum vertical velocity  $15.79 \text{ m s}^{-1}$ .  
 (c) Maximum absolute difference 0.04 K. Maximum vertical velocity  $15.70 \text{ m s}^{-1}$ .



(d) Maximum absolute difference 0.74 K. Maximum vertical velocity  $16.84 \text{ m s}^{-1}$ .  
 (e) Maximum absolute difference 1.04 K. Maximum vertical velocity  $17.15 \text{ m s}^{-1}$ .  
 (f) Max absolute difference 1.67 K. Maximum vertical velocity  $16.90 \text{ m s}^{-1}$ .

Figure 3: Potential temperature difference plots at time  $t = 1000 \text{ s}$ . Differences are between the warm rising bubble with no hill and 1000 m high hills of different half-widths. For a) and d)  $a = 3 \text{ km}$ , for b) and e)  $a = 2 \text{ km}$  and for c) and f)  $a = 1 \text{ km}$  wide. a), b), c) are from the Cut-cell model and d), e), f) are from the terrain-following model, BLASIUS. Differences are in K the contour interval is 0.1 K ranging from -1.2 K to 1.7 K. The maximum absolute potential temperature difference is given beneath each subfigure, along with the maximum vertical velocity.

## Rising bubble test conclusions

- The { hill – no-hill } differences (T & w) with the cut cell model are an order of magnitude smaller than those from the BLASIUS model. They do not become larger as  $h_0/a$  increases from  $1/3^{\text{rd}}$  to  $1/2^{\text{th}}$  to 1.
- The BLASIUS differences increase as the aspect ratio increases, from 0.7 K when the ratio is  $1/3^{\text{rd}}$ , to 1.67 K when the aspect ratio is 1; as a consequence of the more distorted grid as the aspect ratio increases. (BLASIUS cannot be guaranteed to converge with an aspect ratio greater than 1).
- The cut cell results are not affected, and can be run up to an aspect ratio of 10 and (not shown here) show little change in magnitude of temperatures and velocities.

# Conclusions

In these idealised tests

- The cut cell model can accurately simulate the resting atmosphere case, and does not exhibit spurious grid induced winds.
- For the tracer bubble advection test over the tops of mountains, the cut cell model does not exhibit errors aloft induced by the underlying terrain.
- For the rising bubble test, the cut cell model is better at handling steep gradients. The differences due to the underlying terrain do not erroneously increase as the aspect ratio increases.
- For the bubble tests with steep orography (up to an aspect ratio of 10), the results show the cut cell model is stable, without compromising accuracy.
- Issues remain as regards the limitations of small cut cells, and work is being completed on implicit / semi-implicit formulations.





**National Centre for  
Atmospheric Science**  
NATURAL ENVIRONMENT RESEARCH COUNCIL

[www.ncas.ac.uk](http://www.ncas.ac.uk)



## Abstract

Several tests of a model with a cut-cell representation of orography are presented: a resting atmosphere test, advection across a hill and a warm rising bubble over hills with different gradients. The tests are compared with results from terrain-following models.

Results indicate that errors associated with terrain-following coordinates are reduced, in some cases greatly reduced, with the cut-cell approach. In a resting atmosphere the cut-cell approach does not generate flow around an isolated hill however steep the terrain.

Relative errors in a rising bubble test are an order of magnitude smaller than terrain-following simulations. These rising bubble tests demonstrate that the Cut-cell model is better at handling steep gradients than the basic terrain-following method. Differences due to the effect of the underlying terrain do not erroneously increase as the aspect ratio increases in contrast to a terrain-following model.

All these tests demonstrate that by avoiding any distortion of the computational grid away from the terrain, the cut-cell method reduces errors in the flow aloft compared to terrain-following methods. Furthermore, results from the rising bubble test with very steep orography (aspect ratio of 10) demonstrate that the Cut-cell model is stable, without compromising accuracy.